SPACEBORNE AUTONOMOUS AND GROUND BASED RELATIVE ORBIT CONTROL FOR THE TERRASAR-X/TANDEM-X FORMATION[1]

J. S. Ardaens(1), S. D'Amico(1), B. Kazeminejad(1), O. Montenbruck(1), E. Gill(2)

(1)German Space Operations Center (DLR/GSOC, 82234 Wessling, Germany)
E-Mail: jean-sebastien.ardaens@dlr.de
(2) Delft University of Technology (DEOS), Kluyverweg 1, 2629 HS Delft, The Netherlands

Introduction

TerraSAR-X (TSX) and TanDEM-X (TDX) are two advanced synthetic aperture radar (SAR) satellites flying in formation. SAR interferometry allows a high resolution imaging of the Earth by processing SAR images obtained from two slightly different orbits. TSX operates as a repeat-pass interferometer in the first phase of its lifetime and will be supplemented after two years by TDX in order to produce digital elevation models (DEM) with unprecedented accuracy. Such a flying formation makes indeed possible a simultaneous interferometric data acquisition characterized by highly flexible baselines with range of variations between a few hundreds meters and several kilometers [1]. TSX has been successfully launched on the 15th of June, 2007. TDX is expected to be launched on the 31st of May, 2009.

A safe and robust maintenance of the formation is based on the concept of relative eccentricity/inclination (e/i) vector separation whose efficiency has already been demonstrated during the Gravity Recovery and Climate Experiment (GRACE) [2]. Here, the satellite relative motion is parameterized by mean of relative orbit elements and the key idea is to align the relative eccentricity and inclination vectors to minimize the hazard of a collision. Previous studies have already shown the pertinence of this concept and have described the way of controlling the formation using an impulsive deterministic control law [3]. Despite the completely different relative orbit control requirements, the same approach can be applied to the TSX/TDX formation.

The task of TDX is to maintain the close formation configuration by actively controlling its relative motion with respect to TSX, the leader of the formation. TDX must replicate the absolute orbit keeping maneuvers executed by TSX and also compensate the natural deviation of the relative e/i vectors. In fact the relative orbital elements of the formation tend to drift because of the secular non-keplerian perturbations acting on both satellites. The goal of the ground segment is thus to regularly correct this configuration by performing small orbit correction maneuvers on TDX. The ground station contacts are limited due to the geographic position of the station and the costs for contact time. Only with a polar ground station a contact visibility is possible every orbit for LEO satellites. TSX and TDX use only the Weilheim ground station (in the southern part of Germany) during routine operations. This station allows two scheduled contact per day for the nominal orbit configuration, meaning that the satellite conditions can be checked with an interval of 12 hours. While this limitation is usually not critical for single satellite operations, the visibility constraints drive the achievable orbit control accuracy for a LEO formation if a ground based approach is chosen. Along-track position uncertainties and maneuver execution errors affect the relative motion and can be compensated only after a ground station contact.

In order to ease on-ground operations and make maximum reuse of the available on-board resources, the TDX spacecraft will be complemented with an Autonomous Formation Flying (TAFF) system. As outlined in the paper, the objective of TAFF is to mainly provide onboard TDX a robust control algorithm for formation keeping and demonstrate a substitution of ground-based formation control by a space-borne autonomy function. The relative orbit solution is determined from the navigation solutions provided by two synchronized GPS receivers onboard TSX and TDX. Information about TSX is transmitted to TDX through the Inter-Satellite Link (ISL). The on-board navigation module uses an extended Kalman filter and can cope with ISL data gaps of maximum 15 minutes. The expected navigation accuracy is at the meter level. Overall, tasks like orbit determination and control that are traditionally performed on-ground will be transferred to the spacecraft to enable improved relative orbit control performances. Since the orbit control maneuvers are planned and executed more frequently, typically every 3-5 hours, the autonomously controlled formation remains closer to the nominal configuration. The resulting control error is expected to be ten times better (i.e. 20 m, 3D, 1σ) than via ground-

[1] The TanDEM-X project is partly funded by the German Federal Ministry for Economics and Technology (Förderkennzeichen 50 EE 0601) and is realized in a public-private partnership by DLR e.V. and Astrium EADS

based control. The adoption of an autonomous orbit control system on TanDEM-X will enhance the quality of the scientific data products and, on the long-term, reduce the required ground support and the associated costs.

The paper addresses the design of the relative orbit control system for the TSX/TDX formation by comparing space-borne autonomous and ground-based relative orbit control. While the TAFF system development is mainly driven by the limited resources available on the on-board computer and by the requirement of simplicity and robustness, the ground-in-the-loop orbit control has to overcome the limitations given by orbit prediction accuracy and ground-contact latencies. After a detailed description of the e/i vector separation concept and the maneuver planning strategy, the paper analyses the relative orbit control accuracy paying special attention to the simulation environment. To that end, non-keplerian perturbations as well as sensors and actuators are precisely modeled. The simulation environment is designed to investigate the robustness of the control system. Overall the paper presents the resulting strategy and shows how a harmonious integration of autonomous and ground-based orbit control can be achieved through the synergy of space- and ground-segments.

1 Description of the formation

1.1 Relative motion

The relative motion of two bodies can be rigorously described by integrating numerically the equations of motions taking all the relevant perturbations into account. The relative motion is then obtained by computing the difference between the two trajectories. In the present study, we take advantage of the fact that the two satellites are flying on two near-circular orbits in a close formation to derive an analytical expression of the relative motion.

The relative motion is described using the relative orbital elements which provide, if compared with a pure Cartesian description, a better insight into the geometry of the relative trajectory. The description of the motion of spacecraft-2 (i.e. TSX in the sequel) with respect to spacecraft-1 (i.e. TDX in the sequel) requires the definition of the vector $\Delta\boldsymbol{\alpha}$ of relative orbital elements. Based on the Keplerian orbital elements of the two spacecrafts (identified by the subscript k=1,2): a_k semi-major axis, e_k eccentricity, i_k inclination, ω_k argument of perigee, ,Ω_k right ascension of the ascending node and M_k mean anomaly, the relative eccentricity vector $\Delta\boldsymbol{e}$ and the relative inclination vector $\Delta\boldsymbol{i}$ can be defined as

$$\Delta\boldsymbol{e} = e_2\begin{pmatrix}\cos\omega_2\\ \sin\omega_2\end{pmatrix} - e_1\begin{pmatrix}\cos\omega_1\\ \sin\omega_1\end{pmatrix} \tag{1}$$

and

$$\Delta\boldsymbol{i} = \begin{pmatrix} i_2 - i_1 \\ (\Omega_2 - \Omega_1)\sin i_1\end{pmatrix} = \begin{pmatrix}\Delta i \\ \Delta\Omega\sin i_1\end{pmatrix}. \tag{2}$$

Depending on the specific application, either a Cartesian or a polar representation of these vectors is preferable, for which the following notation is employed

$$\Delta\boldsymbol{e} = \begin{pmatrix}\Delta e_x\\ \Delta e_y\end{pmatrix} = \delta e\begin{pmatrix}\cos\varphi\\ \sin\varphi\end{pmatrix} \tag{3}$$

and

$$\Delta\boldsymbol{i} = \begin{pmatrix}\Delta i_x\\ \Delta i_y\end{pmatrix} = \delta i\begin{pmatrix}\cos\theta\\ \sin\theta\end{pmatrix} \tag{4}$$

where δe and φ are the magnitude and the phase of $\Delta\boldsymbol{e}$ whereas δi and θ are the magnitude and the phase of $\Delta\boldsymbol{i}$. The complete set of relative orbital elements is defined as follows

$$\Delta\boldsymbol{\alpha} = \begin{pmatrix}\Delta a\\ a_1\Delta e_x\\ a_1\Delta e_y\\ a_1\Delta i_x\\ a_1\Delta i_y\\ a_1\Delta u\end{pmatrix} = \begin{pmatrix} a_2 - a_1 \\ a_1(e_2\cos(\omega_2) - e_1\cos(\omega_1)) \\ a_1(e_2\sin(\omega_2) - e_1\sin(\omega_1)) \\ a_1(i_2 - i_1) \\ a_1(\Omega_2 - \Omega_1)\sin(i_1) \\ a_1(u_2 - u_1)\end{pmatrix} \tag{5}$$

where the usage of the mean argument of latitude $u = \omega + M$, has been preferred to the usage of the mean anomaly in the case of near circular orbits. The angular differences have been multiplied by the semi-major axis to favor the intuitive representation of the formation geometry. Since the two satellites are flying in close formation, a_1 is simply denoted as a in the sequel.

The description of the relative motion of TSX with respect to TDX is done in the Hill's local co-moving triad ($\boldsymbol{e}_R$,$\boldsymbol{e}_T$,$\boldsymbol{e}_N$) with origin at the center of mass of TDX. The unit vector $\boldsymbol{e}_R$ is aligned with the radial direction,

positive outwards, $\boldsymbol{e}_N$ is aligned with the angular momentum of the satellite, whereas $\boldsymbol{e}_T$ completes the triad. The three unit vectors are defined as follows

$$\boldsymbol{e}_R = \frac{\boldsymbol{r}}{|\boldsymbol{r}|};\ \boldsymbol{e}_N = \frac{\boldsymbol{r}\times\boldsymbol{v}}{|\boldsymbol{r}\times\boldsymbol{v}|};\ \boldsymbol{e}_T = \boldsymbol{e}_N \times \boldsymbol{e}_R . \tag{6}$$

Here $\boldsymbol{r}$ is the position of TDX, $\boldsymbol{v}$ its velocity in an inertial reference frame. The relative position $\Delta\boldsymbol{r}=\boldsymbol{r}_2-\boldsymbol{r}_1$ mapped in this frame may be written as

$$\Delta\boldsymbol{r} = \Delta r_R \boldsymbol{e}_R + \Delta r_T \boldsymbol{e}_T + \Delta r_N \boldsymbol{e}_N . \tag{7}$$

Since the two spacecraft are flying in close formation on near circular orbits, the Hill-Clohessy-Wiltshire (HCW) equations [6], [7] for relative motion can be used. The solution of the HCW equations can be expressed in terms of relative orbital elements as follows [2]

$$\begin{pmatrix}\Delta r_R\\ \Delta r_T\\ \Delta r_N\end{pmatrix} = \begin{bmatrix} 1 & -\cos u & -\sin u & 0 & 0 & 0\\ -\frac{3}{2}(u-u_0) & 2\sin u & -2\cos u & 0 & \cot i & 1\\ 0 & 0 & 0 & \sin u & -\cos u & 0\end{bmatrix}\begin{pmatrix}\Delta a\\ a\Delta e_x\\ a\Delta e_y\\ a\Delta i_x\\ a\Delta i_y\\ a\Delta u\end{pmatrix}. \tag{8}$$

As a consequence, the relative trajectory induced by a non-vanishing relative eccentricity vector with all other relative orbital elements set to zero is an ellipse of semi-minor axis aδe in radial direction and semi-major axis 2aδe in along-track direction. Likewise, a pure difference of relative inclination vector results in harmonic oscillation in the cross-track direction. Figure 1 depicts the relative motion induced by relative e- and i- vectors when Δa=0, Δu=-(Ω_2 - Ω_1)cos(i) and $\theta=\varphi$.

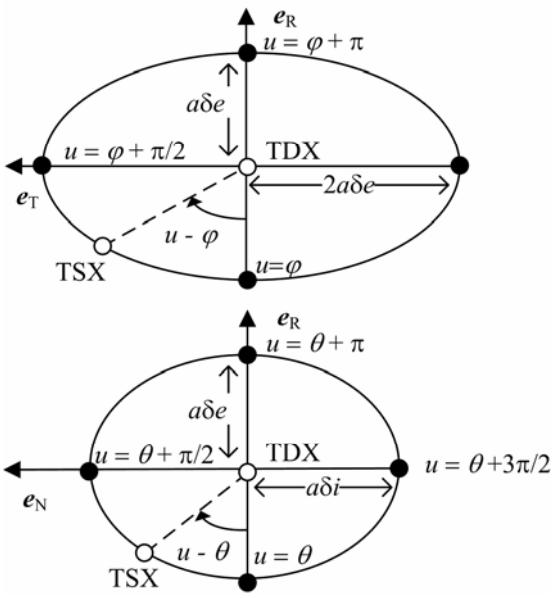

Figure 1: Relative motion of TSX with respect to TDX for aligned e/i vectors: in-plane (top) and out-of-plane (bottom) motion in the Hill frame.

1.2 Perturbations of the formation

Since the Earth is not a perfect sphere, the orbital elements of a LEO satellite are affected by various perturbations [4]. While the periodic perturbations affecting the relative orbital elements of satellites flying in close proximity are mainly cancelled, it remains a secular change of the relative e- and i- vectors. Ignoring the short periodic perturbations, the relative eccentricity vector $\Delta\mathbf{e}$ becomes a time-dependent quantity

$$\Delta\boldsymbol{e} = \delta e\begin{pmatrix}\cos(\varphi_0+\dot{\varphi}t)\\ \sin(\varphi_0+\dot{\varphi}t)\end{pmatrix}. \tag{9}$$

The TSX/TDX formation is flying at an altitude of 514 km on an orbit with an inclination of i=97.42°. As a consequence, $\dot{\varphi}$ is negative and the relative eccentricity vector rotates clockwise over the time. The associated period depends on the orbital period T of the satellite, on the second order zonal coefficient J_2 and on the equatorial radius of the Earth $R_\oplus$ as follows [4]

$$T_G = \frac{2\pi}{|\dot{\varphi}|} \approx \frac{4}{3}\frac{a^2}{R_\oplus^2}\frac{T}{J_2\left|5\cos^2 i - 1\right|}. \tag{10}$$

According to eq. (10), T_G amounts to roughly hundred days. The relative inclination vector is similarly affected by a secular change due to J_2 that causes a secular shift of the orbital planes and thus a linear drift of the Δi_y component

$$\Delta \boldsymbol{i} = \begin{pmatrix} \Delta i \\ \Delta\Omega_0 \sin i - \dfrac{3\pi}{T} J_2 \dfrac{R_\oplus^2}{a^2} \sin^2 i \cdot \Delta i \cdot t \end{pmatrix}. \tag{11}$$

Equation (11) shows that the drift rate of the relative inclination vector depends directly on the inclination difference $\Delta i = i_2 - i_1$. In addition to the secular changes of relative e/i-vectors, other perturbations contribute to altering the relative semi-major axis Δa as well as the relative argument of latitude Δu. The main contribution is due to the differential atmospheric drag, since the two spacecraft have slightly different ballistic coefficients.

1.3 Design of the formation using relative e/i -vectors

The TanDEM-X formation has been designed using the e/i-vector separation concept, which has firstly been developed for the safe collocation of geostationary satellites [5]. This theory is a powerful tool that allows building a close formation of satellites which fulfills the challenging baseline required by the SAR interferometry while minimizing the hazard of a collision.

First of all, a formation is configured by setting properly the relative orbital elements $\Delta\boldsymbol{\alpha}$ between the two spacecrafts. If the relative orbital elements remain constant and Δa is set to zero, the resulting relative motion is a 3D-ellipse, as seen before. The key idea of the e/i separation concept resides in the fact that the position of a satellite can be predicted with a good accuracy in radial and cross-track directions, whereas the prediction is affected by large uncertainties in along-track direction. Indeed, because of the coupling between relative semi-major axis and relative argument of latitude, small errors affecting the initial position and velocity will result in a secular grow of the errors in along-track direction mainly. In addition, maneuver execution errors and small perturbations like atmospheric drag introduce large uncertainties in along-track direction for predictions over large time spans. As a consequence, the relative motion between TSX and TDX can only be considered safe if a minimum separation perpendicular to the flight direction (i.e. in the ($\boldsymbol{e}_R$,$\boldsymbol{e}_N$) plane) is ensured at all times.

This can be achieved by a parallel (or anti-parallel) alignment of the relative eccentricity and inclination vectors. In such a configuration, the minimum radial separation is reached when the cross-track separation is maximal and vice-versa… The separation perpendicular to the flight direction is always bigger than min(aδe,aδi) if the relative semi-major axis is set to zero. For the TSX/TDX mission, the minimum separation perpendicular to the flight direction is required not to be smaller than 250 m. On the contrary, if the two vectors are perpendicular, then the radial and cross-track separations vanish at the same time. In this case, the risk of collision is maximal especially if the along-track errors are high.

Having in mind these considerations, the configuration of the TanDEM-X formation can be easily planned. The relative semi-major axis Δa is nominally zero und should always be kept as small as possible since a non-vanishing Δa induced a drift of the relative mean argument of latitude. The modulus of the relative eccentricity vector is limited by the minimum radial separation necessary for safe proximity operation and by the maximum along-track separation required by interferometry, i.e. 200m $< a\delta e <$500m. The modulus of the relative inclination vector follows the same safety requirements and operational constraint, i.e. 200m $< a\delta i <$500m. In order to avoid a secular drift of the Δi_y component, the inclination difference is set to zero, so that $i_1 = i_2$. The relative inclination vector has thus a phase angle of $\theta = \pm\pi/2$. The relative eccentricity vector should be closely aligned to the relative inclination vector, so that the nominal values are:

$$\Delta \boldsymbol{e} = \delta e \begin{pmatrix} 0 \\ \pm 1 \end{pmatrix} \qquad \text{and} \qquad \Delta \boldsymbol{i} = \delta i \begin{pmatrix} 0 \\ \pm 1 \end{pmatrix}. \tag{12}$$

2 Theory of the formation keeping

2.1 Impulsive maneuver strategy

As outlined before, various perturbations alter the nominal configuration. The most critical is the clockwise drift of $\Delta\mathbf{e}$ that tends to bring the relative eccentricity vector perpendicular to the relative inclination vector, or in other words tends to increase the collision risk. As a consequence, the formation must be controlled to maintain the predefined orientation of the two vectors.

TSX is the leader of the formation. The absolute orbit control performed on ground keeps its orbit close to the nominal orbit. In order to keep the configuration of the formation unchanged, TDX must of course replicate all the commands for absolute orbit keeping performed by TSX. In addition, TDX performs a relative orbit control, i.e. small maneuvers are executed in order to correct the natural drift of the relative orbital elements as well as the other perturbations.

Different control strategies are conceivable. Since no maneuver can be done during a SAR data take, the thruster activities must be as limited as possible. Driven by this operational constraint, the retained approach uses a pair of impulsive maneuvers that regularly corrects the perturbed relative orbital elements.

Let $\Delta\mathbf{v} = (\Delta v_R, \Delta v_T, \Delta v_N)$ denotes a velocity change caused by an impulsive maneuver executed by TDX and mapped in the $(\boldsymbol{e}_R, \boldsymbol{e}_T, \boldsymbol{e}_N)$ frame defined by Eq. (6). The simplified Gauss equations, adapted to near circular non-equatorial orbits [8], indicate how the orbital relative elements of TSX w.r.t. TDX are altered by this maneuver

$$\delta\Delta\boldsymbol{\alpha} = \begin{pmatrix} \delta\Delta a \\ a\delta\Delta e_x \\ a\delta\Delta e_y \\ a\delta\Delta i_x \\ a\delta\Delta i_y \\ a\delta\Delta u \end{pmatrix} = -\frac{1}{n}\begin{bmatrix} 0 & 2 & 0 \\ \sin u & 2\cos u & 0 \\ -\cos u & 2\sin u & 0 \\ 0 & 0 & \cos u \\ 0 & 0 & \sin u \\ 0 & -3n(t-t_M) & 0 \end{bmatrix}\begin{pmatrix} \Delta v_R \\ \Delta v_T \\ \Delta v_N \end{pmatrix}. \tag{13}$$

$\delta\Delta\boldsymbol{\alpha}$ is the variation of relative orbital elements induced by the maneuver, n the mean motion of TDX, t_M the time at which the maneuver took place, t the current time and u the mean argument of latitude at t_M. Because of their low efficiency in term of propellant consumption, the radial maneuvers are not used by TDX. Equation (13) indicates that the set $(\Delta a, \Delta\boldsymbol{e}, \Delta u)$ can be treated separately from $\Delta\boldsymbol{i}$ since the equations are uncoupled. Any along-track maneuver performed at the mean argument of latitude u affects Δa, $\Delta\boldsymbol{e}$ and Δu, thus it is impossible to change only one of these variables through one maneuver. For that reason a pair of tangential maneuvers is necessary, and sufficient, to control the relative orbital elements Δa, $\Delta\boldsymbol{e}$ and Δu i.e. to control the in-plane relative motion. If $\delta\Delta\boldsymbol{\alpha}$ is the desired correction of the relative orbital elements, the execution of the following impulsive delta-v maneuvers (indicated by the superscript [1] and [2])

$$\Delta v_T^1 = \frac{v}{4}\left(\left\|\delta\Delta\boldsymbol{e}\right\| + \frac{\delta\Delta a}{a}\right) \quad \Delta v_T^2 = \frac{v}{4}\left(\left\|\delta\Delta\boldsymbol{e}\right\| - \frac{\delta\Delta a}{a}\right), \tag{14}$$

at the following mean argument of latitudes

$$u^1 = \operatorname{atan}\left(\frac{\delta\Delta e_x}{\delta\Delta e_y}\right) \text{ and } u^2 = u_1 + \pi \ , \tag{15}$$

will correct the relative orbital elements Δa and $\Delta\boldsymbol{e}$ as desired. The only parameter that can not be instantaneously corrected is the relative mean argument of latitude Δu. However by setting a non-vanishing relative semi-major axis Δa during a time interval δt, one can induce a variation of Δu

$$\delta\Delta u = -\frac{3}{2}n\delta t\frac{\Delta a}{a}, \tag{16}$$

that can be used to maintain Δu in a tolerance interval centered on a predefined nominal value. The relative inclination vector is simply controlled by one cross-track impulse as follows

$$\Delta v_N = 2\cdot v\cdot\left\|\delta\Delta\boldsymbol{i}\right\| \quad \text{at} \quad u = \operatorname{atan}\left(\frac{\delta\Delta i_x}{\delta\Delta i_y}\right) \ . \tag{17}$$

2.2 In plane control algorithm

This paragraph describes in more details the control feeback law applied to the relative orbital elements governing the in-plane relative motion, i.e. $(\Delta a, \Delta\boldsymbol{e}, \Delta u)$. Let $\Delta\boldsymbol{\alpha}^n$ denote the nominal configuration of the relative orbital elements. The goal of the algorithm is to maintain the actual set of orbital elements $\Delta\boldsymbol{\alpha}$ as close as possible to the nominal configuration. The retain approach consists in performing a set of maneuvers at a regular frequency to maintain the relative orbital elements within a tolerance window centered on their nominal value. The Figure 2 depicts the evolution of the controlled relative orbital elements during a set of maneuvers. The time between each pair of maneuvers is called *maneuver cycle* and is set to an integer number m of orbital periods

$$T_{\text{man}} = m\cdot T \ . \tag{18}$$

In order to simplify the algorithm, the only perturbation that is taken into account is the secular rotation of the relative eccentricity vector due to the Earth's oblateness. The other perturbations, notably the differential drag, have been considered as negligible [3]. Since the control frequency is fixed, it is easy to compute the angular drift of $\Delta\boldsymbol{e}$ during a maneuver cycle. This drift amounts to

$$\delta\varphi = \dot{\varphi}\cdot T_{\text{man}} . \tag{19}$$

As a consequence, the tolerance window for $\Delta\boldsymbol{e}$ is defined as follows. Right before the execution of each pair of maneuvers the relative eccentricity vector reaches its maximum angular deviation, $\delta\varphi^{\max} = \delta\varphi/2$, from the nominal value. The goal of the two maneuvers, separated by half an orbital revolution, is to bring $\Delta\boldsymbol{e}$ back to the opposite side of the tolerance window. The desired relative eccentricity vector after the set of maneuvers is thus:

$$\Delta\boldsymbol{e}^{\text{man}} = \boldsymbol{R}(-\delta\varphi^{\max})\Delta\boldsymbol{e}^{\text{n}} , \tag{20}$$

where $\boldsymbol{R}$ stands for the elementary rotation matrix in the relative eccentricity plane. After the pair of maneuvers, $\Delta\boldsymbol{e}$ will slowly drift to the target relative eccentricity vector at the end of the maneuver cycle given by

$$\Delta\boldsymbol{e}^{\mathrm{t}} = \boldsymbol{R}(\delta\varphi^{\max})\Delta\boldsymbol{e}^{\mathrm{n}}, \tag{21}$$

so that $\Delta\boldsymbol{e}$ is always confined in a tolerance window centered on $\Delta\boldsymbol{e}^{n}$.
The total desired correction of relative eccentricity vector that has to be generated by the pair of maneuvers is expressed as:

$$\delta\Delta\boldsymbol{e} = \Delta\boldsymbol{e}^{\mathrm{man}} - \Delta\boldsymbol{e} \tag{22}$$

where $\Delta\boldsymbol{e}$ represents the current relative eccentricity vector (i.e. before the execution of the first maneuver). The disadvantage of a two-maneuver strategy is that the relative mean argument of latitude undergoes a drift during the two maneuvers. Indeed, the first maneuver sets Δa to a non-vanishing value while the second one brings Δa back to zero for a pure relative eccentricity vector control. The non-zero difference of the semi-major axis between the satellites in between the maneuver pair (i.e. half an orbital revolution) increases considerably the along-track separation. The solution of this problem consists in targeting at the end of the pair of maneuvers a slightly non-vanishing Δa. This will compensate the shift of Δu by introducing a linear counter drift that brings Δu back to its nominal value. Here, a tolerance window is also applied. For small values of $\delta\varphi^{\max}$ (i.e. for short maneuver cycles) the total variation of Δu within the time interval between the two tangential maneuvers is approximately given by

$$a\delta\Delta u_{\Delta v} = \frac{3}{2}T\Delta v \approx \frac{3\pi}{4}a\left(\left\|\Delta\boldsymbol{e}^{\mathrm{man}} - \Delta\boldsymbol{e}^{\mathrm{t}}\right\| + \frac{\Delta a^{t} - \Delta a}{a}\right) \approx \frac{3\pi}{4}\delta\varphi\left\|a\Delta\boldsymbol{e}^{\mathrm{n}}\right\|. \tag{23}$$

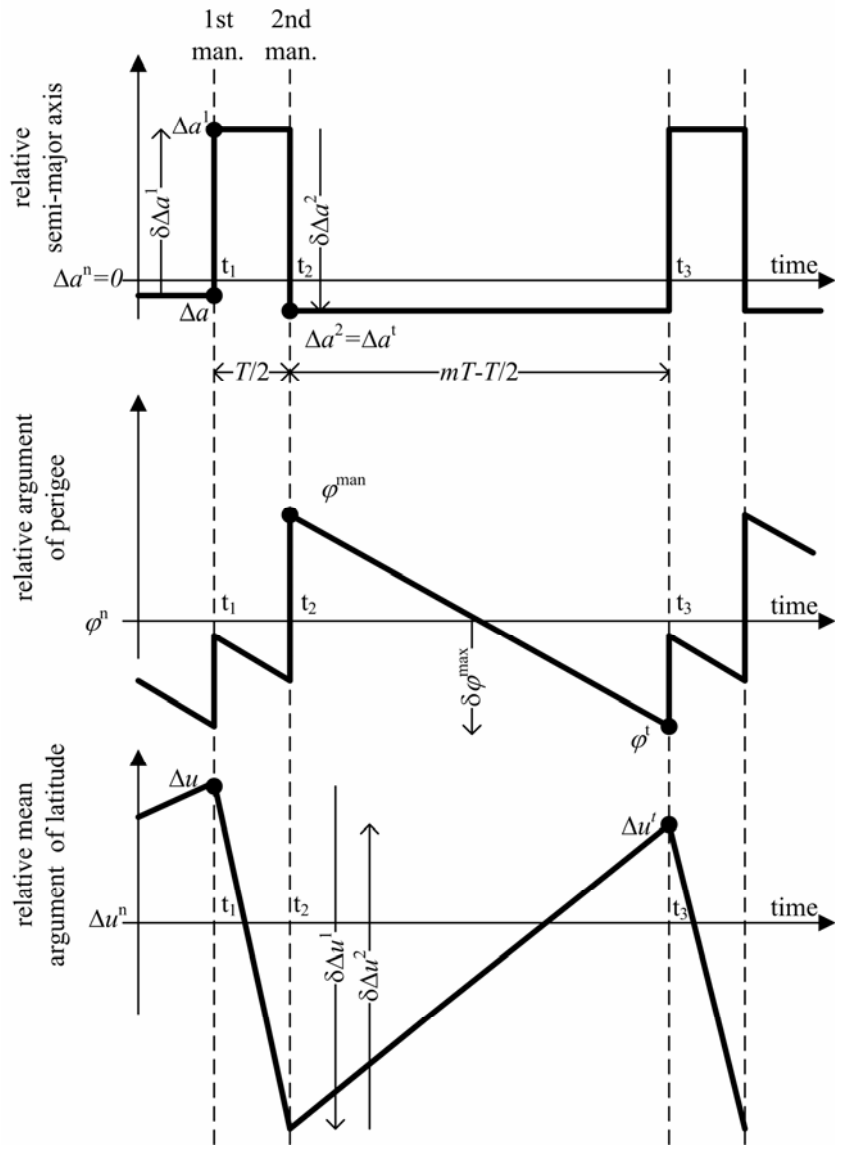

Figure 2: Evolution of the relative semi-major axis, argument of perigee and argument of latitude during the maneuver cycle.

After the pair of maneuvers, Δu reaches one extremity of the tolerance window. A non-vanishing Δa is introduced so that Δu reaches at the end of the maneuver cycle the target value:

$$\Delta u^{t} = \Delta u^{n} + \delta\Delta u_{\Delta v}/2 . \tag{24}$$

As a consequence, the variation of relative mean argument of latitude is always comprised within the tolerance window centered on the nominal value Δu^{n}.

The value of the target relative semi-major axis Δa^{t} that drives the variation of Δu is consequently of importance and must be treated carefully.

Let t_1 denote the time of the execution of the first maneuver and $\Delta\boldsymbol{\alpha}$ the configuration of the formation at time t_1. The first maneuver results in a new value Δa^{1} for the relative semi-major axis until $t_2=t_1+T/2$, time of the second maneuver. The second maneuver results in a new value $\Delta a^{2} = \Delta a^{t}$ (i.e. the target relative semi-major axis at the end of the pair of maneuvers) for the relative semi-major axis until $t_3=t_1+T_{man}$, time of the first maneuver of the next pair of maneuvers.

The total variation of Δu over the maneuver cycle is

$$\delta\Delta u = \Delta u^{t} - \Delta u = \delta\Delta u^{1} + \delta\Delta u^{2} , \tag{25}$$

where $\delta\Delta u^{1}$ is the variation of relative mean argument of latitude introduced by Δa^{1} during $T/2$ and $\delta\Delta u^{2}$ is the one introduced by Δa^{2} during T_{man}-$T/2$. Equation (16) yields

$$\begin{cases} \delta\Delta u^{1} = -\frac{3}{2}\mathrm{n}\frac{T}{2}\frac{\Delta a^{1}}{a} = -\frac{3}{2}\pi\frac{\Delta a^{1}}{a} \\ \delta\Delta u^{2} = -\frac{3}{2}\mathrm{n}\left(\mathrm{T}_{\mathrm{man}} - \frac{T}{2}\right)\frac{\Delta a^{2}}{a} = -3\pi\left(m-\frac{1}{2}\right)\frac{\Delta a^{2}}{a} \end{cases} . \tag{26}$$

Using equations (13) and (14), we can formulate the variation of the relative semi-major axis introduced by the two maneuvers $\delta\Delta a^{1} = \Delta a^{1} - \Delta a$ and $\delta\Delta a^{2} = \Delta a^{2} - \Delta a^{1}$ in function of the desired relative semi-major axis at the end of the pair of maneuver Δa^{t}:

$$\begin{cases} \delta\Delta a^{1} = \Delta a^{1} - \Delta a = -\frac{2}{n}\Delta \boldsymbol{v}_T^{1} = -\frac{a}{2}\left(\left\|\delta\Delta\boldsymbol{e}\right\| + \frac{\delta\Delta a}{a}\right) \\ \delta\Delta a^{2} = \Delta a^{2} - \Delta a^{1} = -\frac{2}{n}\Delta \boldsymbol{v}_T^{2} = -\frac{a}{2}\left(\left\|\delta\Delta\boldsymbol{e}\right\| - \frac{\delta\Delta a}{a}\right) \end{cases} . \tag{27}$$

Using equation (25),(26),(27), one obtains

$$\begin{aligned} \Delta u^{t} - \Delta u &= \delta\Delta u^{1} + \delta\Delta u^{2} \\ &= -\frac{3\pi}{a}\left(\frac{3\Delta a}{4} - \frac{a}{4}\left\|\delta\Delta\boldsymbol{e}\right\| + \left(m-\frac{3}{4}\right)\Delta a^{t}\right) \end{aligned} . \tag{28}$$

Finally, the variation of semi major-axis necessary to compute the size of the two maneuvers can be computed using this formulation

$$\delta\Delta a = \Delta a^{t} - \Delta a = \left(-\frac{\left(\Delta u^{t} - \Delta u\right)a}{3\pi} - m\Delta a + \frac{a\left\|\delta\Delta\boldsymbol{e}\right\|}{4}\right)\cdot\frac{1}{m-\frac{3}{4}} . \tag{29}$$

3 Operational implementation

The TSX spacecraft is equipped with a hydrazine mono-propellant propulsion system. The actuators are arranged in two branches with four 1 N thrusters each and will be used for the absolute orbit maintenance maneuvers. Apart from two major modifications, TDX is a 1:1 rebuild of TSX. This ensures operational compatibility and guarantees minimum impact on the present TSX design. TSX will continuously send House-Keeping telemetry data in S-band. TDX will receive TSX telemetry by using an additional S-band receiver system. Secondly the tight requirements on the relative orbit control have imposed an adaptation of the propulsion system. TDX has been equipped with a new cold gas system dedicated to relative orbit control maneuvers. The additional propulsion system is composed of two branches of four 40mN thrusters pointing in flight and anti-flight direction. This choice will guarantee the availability of appropriate thrusters for relative orbit control, and a quasi-identical execution of orbit maintenance maneuvers by the two spacecrafts.

Two kinds of operational implementations are envisaged. In the first mission phase, formation acquisition, maintenance and reconfiguration will be performed by the flight dynamics team on ground. Step by step, the on-board autonomous controller will be activated, tested and validated. Even if its design is as simple as possible, the fully autonomous onboard control will improve drastically the control performances (by a factor of 10) and ease the ground operations.

3.1 Ground-in-the-loop orbit control

The space segment consists mainly of the TDX and TSX spacecraft and provides GPS data (e.g. navigation solution, code and carrier phase measurement) and AOCS housekeeping data to the ground segment during ground station contacts. These data are used to perform a very accurate orbit determination to get the best possible knowledge of the satellite status and motion, using up-to-date solar flux data, Earth rotation parameters and a precise modeling of the physical forces. The controller compares the predicted orbit parameters over 24 h with the nominal one and calculates a time tagged maneuver, which is uploaded during the next ground station contact.

The main limitation of a ground-in-the-loop orbit control is due to the limited number of ground stations, and thus the limited visibility of the LEO formation. The TanDEM-X mission will use only the Weilheim ground station (in the southern part of Germany) during routine operations. This station allows two scheduled contacts per day. As a consequence, the size of the tolerance window within which the relative orbital elements are confined is relatively large. In addition, the small execution errors of the thrusters can be compensated only after 1 day. Considering a hydrazine maneuver for orbit maintenance of 5 cm/s executed simultaneously by TSX and TDX, the expected thruster precision on each spacecraft of 2% can induce a difference of 0.25 mm/s, which results in a change of relative semi-major axis of about 0.5 m. Such a difference causes an along-track drift of roughly 75 m in a day, which leads to severe limitations in terms of control performances in along-track direction. The only way to improve the control performance is to reduce the maneuver cycle, which can be easily done in an onboard autonomous orbit control.

3.2 TanDEM-X Autonomous Formation Flying.

The TanDEM-X Autonomous Formation Flying (TAFF) subsystem will reside on the TDX onboard computer as part of the Attitude and Orbit Control System (AOCS). TAFF gets as input the GPS navigation solutions provided by the GPS receiver onboard TDX and, through an Inter-Satellite Link (ISL), also from the GPS receiver onboard TSX. TAFF will process the input measurements in a relative navigation filter and, based on the guidance law described before, compute the cold gas thruster commands for autonomous formation flying.

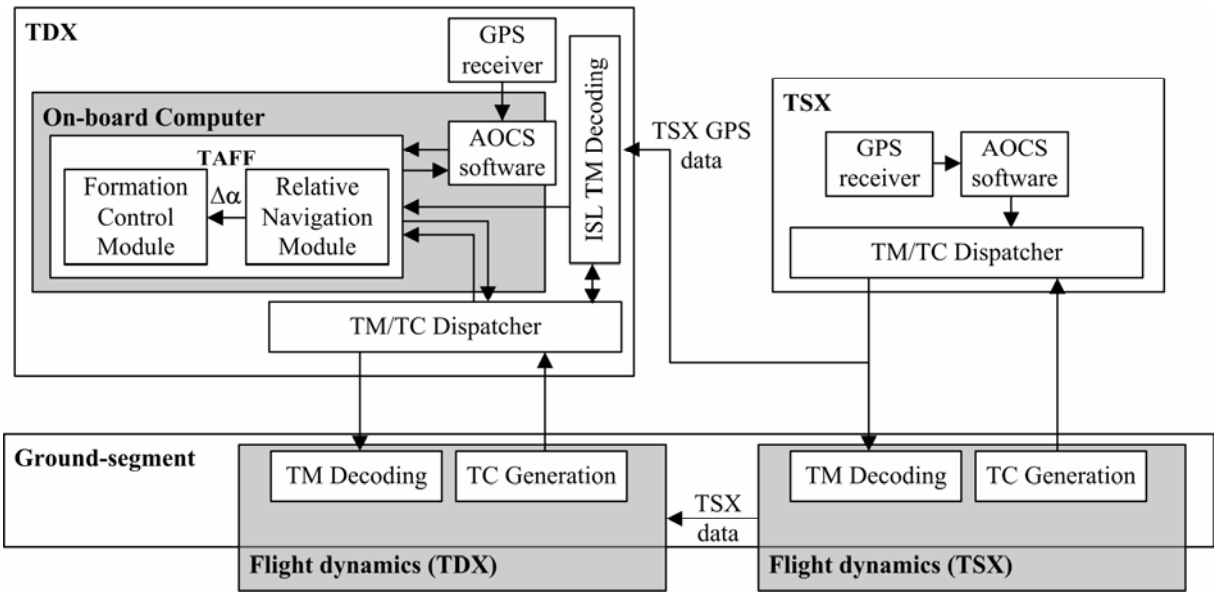

Figure 3: Schematic functional view of TAFF.

As depicted in Figure 3, TAFF is structured into two main parts: the Relative Navigation and the Formation Control Modules. The Relative Navigation Module aims at providing a filtered solution of the current relative orbital elements. The Formation Control Module commands the thrusters of TDX to correct the relative orbital elements of the formation. The performance is however limited by the noisy input of the controller, i.e. the relative navigation solution, which is not as accurate as what can be achieved on ground. Indeed, because of the limited onboard resources, a simple analytical model is used to compute the relative orbital elements with an accuracy of several meters.

3.3 Integration of autonomous control within the TanDEM-X mission

One of the most challenging tasks in the design of TAFF is its harmonious integration within space- and ground-segments. TAFF is supposed to be an experimental add-on and shall not perturb or compromise the proper functioning of the TanDEM-X mission. The following aspects shall be handled with special care.

First of all the TanDEM-X mission will realize the first GPS-based fully autonomous formation flying of close LEO spacecraft in Europe. Due to the lack of experience in operating closely flying LEO satellites, TAFF will be

activated gradually. To that purpose, the software has been designed to support four operational modes: off, navigation-only, open-loop and closed-loop. The first testing phase will assess the in-flight performance of the navigation module. The Relative Navigation Module must be robust and reliable in all conditions, and must autonomously detect any potential problem. Since the Formation Control Module relies on the information of the Relative Navigation Module, this phase is critical. Afterwards, TAFF will be switched to open-loop mode. In this mode, the control module is activated, computes the necessary maneuvers but the maneuvers are not executed. Extended monitoring and analysis using telemetry is then performed to assess the behavior of the algorithm in real conditions. If these two phases are successful, TAFF will be then switched to closed-loop mode, launching the first European experience in terms of autonomous formation flying.
The autonomous triggering of maneuvers undergoes some major operational constraints. No maneuver can be executed during Digital Elevation Model (DEM) acquisition and along-track interferometry campaigns, in addition no relative orbit control maneuvers can be executed in the vicinity of a ground planned maneuver. By design, the maneuvers will take place when no DEM acquisition is performed. Since the along-track interferometry campaigns are not routine events, it has been chosen that the control module of TAFF will be switched off by the ground segment as part of a procedure when performing such a campaign.
In order to avoid any interference between ground-planned maneuvers for absolute orbit control and autonomously issued maneuvers for relative orbit control, a list of the planned maneuvers will be routinely uploaded to TAFF at each ground contact. Internally TAFF will prevent the generation of cold gas thruster activations within a predefined exclusion window centered on the execution time of a ground planned maneuver.

4 Numerical simulations

4.1 Simulation environment

The objective of the simulations is to demonstrate the proper functioning of TAFF, but especially to evaluate and assess the performance of the two implementations: on-board and ground-in-the-loop.
For this purpose, an accurate simulation environment has been developed and set up. The Figure 4 represents the simulation environment. The position and velocity of the two spacecrafts are computed by integrating numerically the equations of motions. A very accurate dynamical model has been used to that end, comprising the Earth gravity model GGM01S up to the degree of 30, the tidal perturbations, the luni-solar perturbations, the relativistic effects, the atmospheric drag (using the Jacchia atmospheric model) and the solar radiation pressure (using a classical cannon ball model).

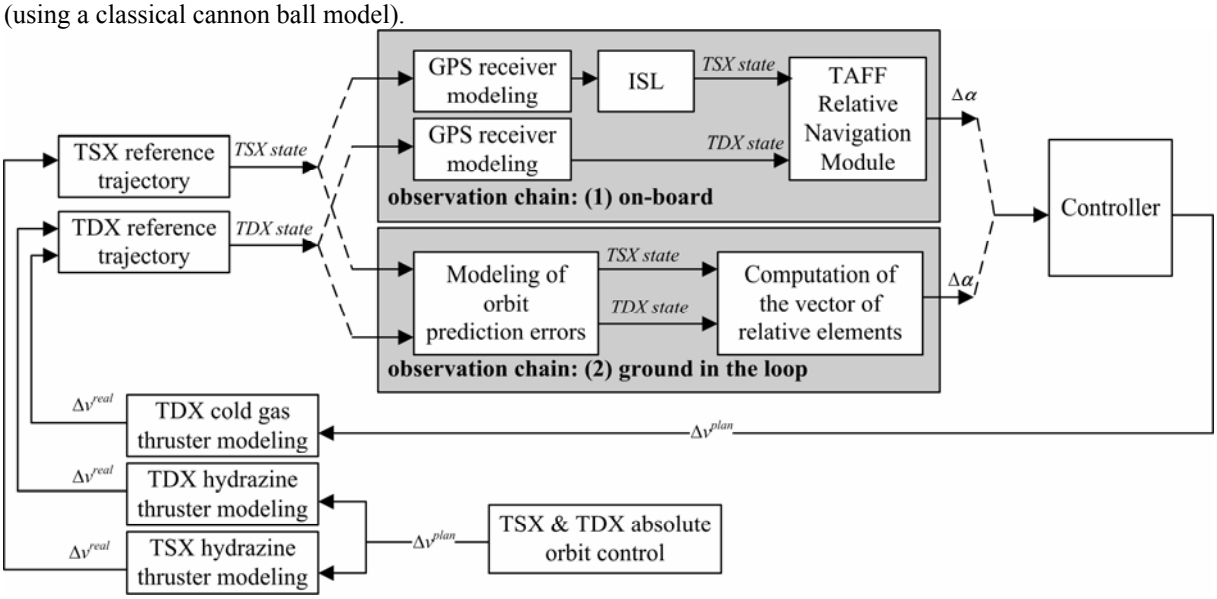

Figure 4: Schematic functional the simulation environment. The relative navigation sensor is modeled differently for ground-in-the-loop and autonomous control.

The states of the two spacecrafts feed the observation chain that aims at computing the current relative orbital elements of the formation. This chain provides to the controller a set of relative orbital elements that is affected by errors and thus tends to degrade the performances of the controller. In the onboard implementation, the observation chain is composed of the GPS receivers onboard TDX and TSX, the ISL and the Relative Navigation Module of TAFF. The accuracy of this chain amounts to about 2m R.M.S. Since the errors affecting the relative navigation depend on the behavior of the receiver, on the possible data gaps of the ISL and on the algorithm used in the Relative Navigation Module of TAFF, they have a specific pattern and can not be assimilated to a purely Gaussian noise. As a consequence, it is mandatory to implement the complete chain

instead of using a random noise generator. To that end, the behavior of the GPS receivers has been precisely modeled. In addition, short sporadic interruptions (less than 15 minutes) of the ISL are modeled.
In the ground-in-the-loop implementation, the orbit determination is very accurate but since the ground control is not done in real time, the relative orbital elements at the time of the maneuver must be predicted. This induces an additional error that amounts to some meters over 1 day. These errors have been modeled via a Gaussian noise. The Table 1 reports the accuracy of the onboard and ground-in-the-loop observation chains.

Table 1: Accuracy of the modeled sensors

Relative navigation accuracy[m]						
	radial		tangential		cross-track	
	mean	σ	mean	σ	mean	σ
on-board observation chain (1)	0.3	1.5	0.2	3.2	-0.3	0.9
ground in the loop observation chain (2)	0.0	0.2	8.0	3.0	0.0	1.0

The output of the observation chain is then used by the controller that implements the algorithm described above. The maneuver commands sent by the controller are then converted into a thrust. The ground planned maneuvers have been also modeled in order to study the stability of the controller in the case of unexpected perturbations of the formation. To that end, a tangential maneuver of 5 cm/s executed on both TSX and TDX is executed every two days during the simulation. The performances of the thrusts have been as well precisely modeled. The execution of a maneuver is indeed affected by two errors: an error η on the size of the thrust and an error on its orientation (σ_{roll}, σ_{pitch} and σ_{yaw} errors). Since the cold gas and hydrazine propulsion systems are quite different, different settings were necessary for the hydrazine and cold gas thrusters. Table 2 summarizes the values adopted for the actuators. The orbit propagator of TDX and TSX are finally fed with the aforementioned thrusts. In order to improve the realism of the simulation, the maneuvers are not considered in the orbit propagation as impulsive but as extended, i.e. the resulting thrust is numerically integrated over the burn duration.

Table 2: Modeling parameters of the actuators

Propulsion system accuracy				
	η[%]	roll[°]	pitch [°]	yaw[°]
Cold gas thruster	3.0	0.0	0.0	1.0
Hydrazine thruster	2.0	0.0	0.0	0.0

The configuration of the formation is set as follows in [m]:

$$\Delta a = 0 \quad a\Delta \boldsymbol{e} = \begin{pmatrix} 0 \\ 300 \end{pmatrix} \qquad a\Delta \boldsymbol{i} = \begin{pmatrix} 0 \\ 500 \end{pmatrix} \qquad a\Delta u = -\frac{\Delta \mathrm{i}_y}{\operatorname{cotan} i} = 65.29 \,.$$

A differential ballistic coefficient of 2% has been introduced between the two satellites. Since the control algorithm doesn't take the differential drag into account, a control error in along-track direction is expected to be found.

4.2 Ground- in- the- loop versus autonomous control

A 20 day simulation, starting from the 2nd July 2006, has been launched for both ground-in-the-loop and onboard autonomous approaches. Figure 5 and Figure 6 show the evolution of the controlled relative orbital elements in the two cases. Even if they are affected by some perturbations, the behavior of the relative semi-major, relative argument of perigee and relative mean argument of latitude is clearly identifiable from the theoretical description made before. This indicates that the control theory works properly under non-ideal conditions. The dashed vertical lines indicates where ground planned absolute orbit control maneuvers are executed. Even if big errors are introduced, the plots indicate that the control theory is robust enough to cope with such perturbations.
The autonomous control has a maneuver cycle of 2 orbital revolutions whereas the maneuver cycle of a ground in a loop scheme is set to 15 orbital revolutions. From these plots, it is clear that a reduced maneuver cycle provides a much better control accuracy. Firstly, the tolerance window in which the controlled relative elements evolve is much bigger when the maneuver cycle is set to 1 day. Secondly, the reaction time of the relative orbit control system is dramatically shorter with an autonomous controller. In this simulation, the absolute maneuver execution errors cause large drifts of the relative mean argument of latitude. This can be corrected very quickly by the autonomous controller (the controller is activated in the simulation 20 minutes after the performance of a ground planned maneuver), but not in a pure ground-in-the-loop scheme.
The simulation applies a very demanding scenario where absolute maneuvers are performed every 2 days. This is realistic since at the end of the TerraSAR-X mission, absolute orbit maneuvers are expected to be executed on a daily base due to the high solar activity. In this phase, the efficiency of TAFF will be extremely advantageous.
In order to assess systematically the control performance, the actual relative position is compared with the desired relative position (i.e. obtained through the nominal relative orbital elements). Table 3 compares the control accuracy obtained using the two implementations.

Table 3: Achieved control performance over 20 days using autonomous and ground-in-the-loop control

	Control performance [m]					
	radial		along-track		cross-track	
	mean	σ	mean	σ	mean	σ
Autonomous onboard control	0.3	1.7	2.2	6.5	0.3	0.3
Ground-in-the loop control	0.4	5.7	-59.7	89	0.3	0.4

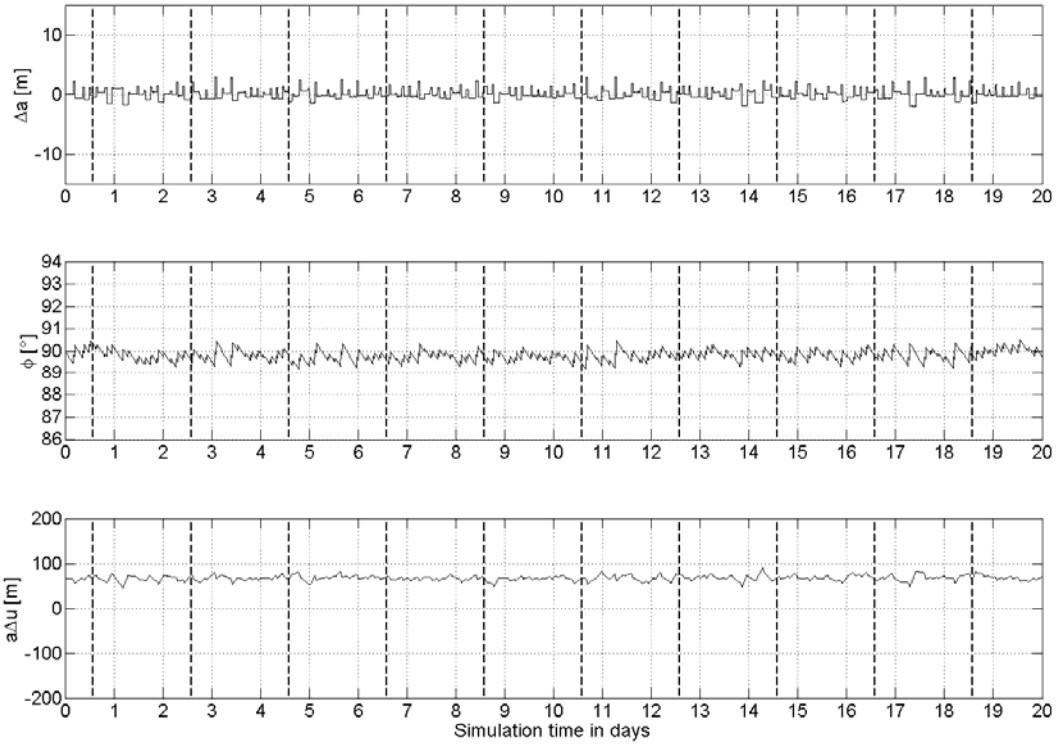

Figure 5: Relative semi-major axis (top), relative argument of perigee (middle) and relative mean argument of latitude (bottom) over 20 days with space borne autonomous relative orbit control of the TSX/TDX formation.

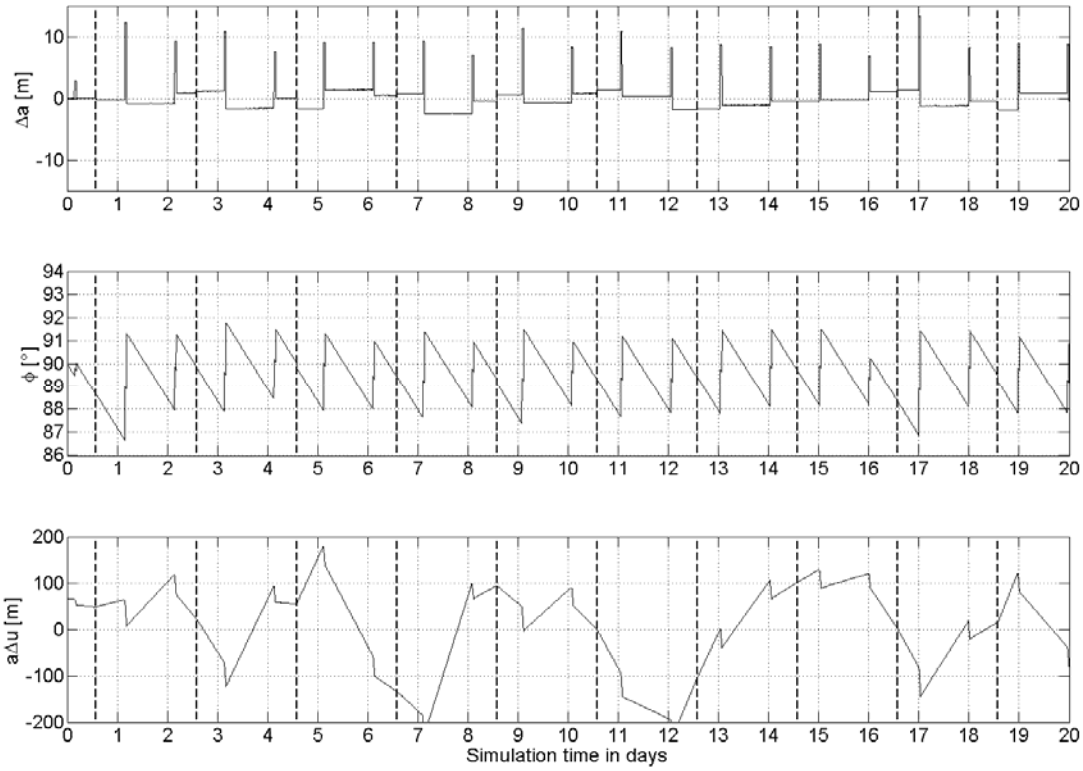

Figure 6: Relative semi-major axis (top), relative argument of perigee (middle) and relative mean argument of latitude (bottom) over 20 days with ground-in-the-loop relative orbit control of the TSX/TDX formation.

5 Conclusion

The parameterization of the relative motion in terms of relative e/i-vectors is a powerful tool enabling the design of safe formations with short separations. The control strategy that has been presented in this paper shows the extreme simplicity and flexibility of the formation keeping approach by applying the same algorithms to a ground-in-the-loop scheme as well as to an autonomous onboard controller.
An analytical model has been adopted for the computation of the target relative orbital elements at the end of the maneuver cycle. In contrast to a real-time application, a severe degradation of the along-track control accuracy is observed for the long maneuver cycles typical of a ground-in-the-loop control scheme. As a consequence, the ground-based control should make use of available high accurate numerical tools to predict the relative position after a pair of maneuvers applying a full dynamical model.
Nevertheless, the ground-in-the-loop control can not overcome its main limitation: the long response time. Despite the availability of an accurate orbit prediction, the ground-based controller suffers from the lack of visibility of the LEO formation flying spacecraft. Thus the tolerance windows around the nominal relative orbital elements are constrained by the large maneuver cycle and several hours are necessary to correct the maneuver execution errors introduced by previous thruster activations. The autonomous onboard controller makes use of a less accurate but continuous navigation solution and can take benefit from a reduced maneuver cycle, allowing high control frequency and short reaction times to provide an orbit control accuracy one order of magnitude better. The real world simulations described in this paper allows a first assessment of the relative orbit control accuracy achievable through the TanDEM-X Autonomous Formation Flying (TAFF) subsystem: 2m (1σ) in radial and cross-track directions and less than 10m (1σ) in along-track direction.

Acronyms and Abbreviations

AOCS	Attitude and Orbit Control Software
ATI	Along-track Interferometry
DLR	Deutsches Zentrum für Luft- und Raumfahrt
DEM	Digital Elevation Model
GPS	Global Positioning System
GSOC	German Space Operations Center
HCW	Hill Clohessy Wiltshire equations
ISL	Inter-Satellite Link
LEO	Low Earth Orbit
OBC	On-Board Computer
SAR	Synthetic Aperture Radar
TAFF	TanDEM-X Autonomous Formation Flying
TC	Telecommand
TM	Telemetry
TDX	TanDEM-X
TSX	TerraSAR-X

References

[1] A. Moreira et al., "TanDEM-X: A TerraSAR-X Add-on Satellite for Single-Pass SAR Interferometry",IGARSS,Achorage,USA,2004

[2] D'Amico S., Montenbruck O.; "Proximity Operations of Formation-Flying Spacecraft Using an Eccentricity/Inclination Vector Separation", Journal of Guidance, Control, and Dynamics, Vol. 29, No. 3, May-June (2006).

[3] D'Amico S., Montenbruck O., Arbinger Ch., Fiedler H., "Formation Flying Concept For Close Remote Sensing Satellites",AAS 05-156,15th AAS/AISS Space Flight Dynamics, 11-15 Oct. 2003,Munich, Germany (2004)

[4] P.Micheau, "Orbit Control Techniques for Low Earth Orbiting (LEO) Satellites", Chap. 13 in Carrou J.P. ed, Spaceflight Dynamics, Cepadues-Editions, Toulouse, France, 1995.

[5] Eckstein M. C., Rajasingh C.K., Blumer P.; Colocation Strategy and Collision Avoidance for the Geostation-ary Satellites at 19 Degrees West; International Symposium on Space Flight Dynamics; 6-10 Nov. 1989, CNES, Toulouse (1989)

[6] Hill G. W.; "Researches in the Lunar Theory", American Journal of Mathematics, Vol. 1, pp. 5-26, (1878).

[7] Clohessy W., Wiltshire R.; "Terminal Guidance Systems for Satellite Rendezvous", Journal of Aerospace Sciences, Vol. 27, pp. 653-658, (1960).

[8] C.Valorge et al, "Processing orbit perturbations", Chap. 6 in Carrou J.P. ed, Spaceflight Dynamics, Cepadues-Editions, Toulouse, France, 1995